

The Shortest Period Detached Binary White Dwarf System^{*}

Mukremin Kilic^{1†}, Warren R. Brown¹, S. J. Kenyon¹, Carlos Allende Prieto^{2,3}, J. Andrews⁴, S. J. Kleinman⁵, K. I. Winget⁶, D. E. Winget⁶ and J. J. Hermes⁶

¹*Smithsonian Astrophysical Observatory, 60 Garden St, Cambridge, MA 02138, USA*

²*Instituto de Astrofísica de Canarias, E-38205 La Laguna, Tenerife, Spain*

³*Departamento de Astrofísica, Universidad de La Laguna, E-38206 La Laguna, Tenerife, Spain*

⁴*Columbia Astrophysics Laboratory, Columbia University, New York, NY 10027, USA*

⁵*Gemini Observatory, 670 N. A'ohoku Place, Hilo HI 96720, USA*

⁶*Dept. of Astronomy, University of Texas at Austin, RLM 16.236, Austin, TX 78712, USA*

16 February 2022

ABSTRACT

We identify SDSS J010657.39–100003.3 (hereafter J0106–1000) as the shortest period detached binary white dwarf (WD) system currently known. We targeted J0106–1000 as part of our radial velocity program to search for companions around known extremely low-mass (ELM, $\sim 0.2M_{\odot}$) WDs using the 6.5m MMT. We detect peak-to-peak radial velocity variations of 740 km s^{-1} with an orbital period of 39.1 min. The mass function and optical photometry rule out a main-sequence star companion. Follow-up high-speed photometric observations obtained at the McDonald 2.1m telescope reveal ellipsoidal variations from the distorted primary but no eclipses. This is the first example of a tidally distorted WD. Modeling the lightcurve, we constrain the inclination angle of the system to be $67^{\circ} \pm 13^{\circ}$. J0106–1000 contains a pair of WDs ($0.17M_{\odot}$ primary + $0.43M_{\odot}$ invisible secondary) at a separation of $0.32R_{\odot}$. The two WDs will merge in 37 Myr and most likely form a core He-burning single subdwarf star. J0106–1000 is the shortest timescale merger system currently known. The gravitational wave strain from J0106–1000 is at the detection limit of the Laser Interferometer Space Antenna (LISA). However, accurate ephemeris and orbital period measurements may enable LISA to detect J0106–1000 above the Galactic background noise.

Key words: (stars:) binaries (including multiple): close — (stars:) white dwarfs — (stars:) individual (SDSS J010657.39–100003.3) — Galaxy: stellar content

1 INTRODUCTION

ELM WDs are ideal targets for finding binary WD merger systems. Short period binary stars interact early in their stellar evolution, experience enhanced mass-loss during one or two common-envelope phases (Sarna et al. 1996), and end up as lower mass WDs. Thus the most compact binary systems are expected to form ELM WDs, and a survey targeting ELM WDs should discover merging systems.

Kilic et al. (2009, 2010, 2011) and Brown et al. (2010) have established a radial velocity program, the ELM Sur-

vey, to search for companions around known ELM WDs in the SDSS Data Release 7 footprint. The discovery of 12 binary WD merger systems in a sample of two dozen WDs observed to date has tripled the number of known binary WD merger systems. Eighteen of the $M \leq 0.25M_{\odot}$ WDs in the ELM Survey are in 1–24 hr period binaries with merger times as short as 100 Myr. Six of these systems have extreme mass ratios ($M_1/M_2 = q \approx 0.2$), which may lead to stable mass transfer AM CVn systems. If the mass-accreting WDs in these systems are massive, they can potentially form Type Ia supernovae (SNe, Webbink 1984; Iben & Tutukov 1984). Alternatively, accretion of helium from a companion may lead to the detonation of the surface helium layer on a C/O WD in a fast and faint supernova, i.e. SNe “Ia” (Bildsten et al. 2007).

Here we present the exciting discovery of a new binary

^{*} Based on observations obtained at the MMT Observatory, a joint facility of the Smithsonian Institution and the University of Arizona.

[†] *Spitzer Fellow*

system found in the ELM survey. J0106–1000 was originally classified as a subdwarf star in the SDSS DR4 WD catalog of Eisenstein et al. (2006). Kleinman (2010) re-classified it as an ELM WD based on a reanalysis of the SDSS spectroscopy. Our follow-up radial velocity and high speed photometric observations demonstrate that J0106–1000 contains a pair of WDs with an orbital period of only 39.1 minutes. This system, the shortest period detached binary WD system known, presents the first detection of a tidally distorted WD.

In Section 2 we describe our spectroscopic and photometric observations. In Sections 3 and 4 we constrain the physical parameters of the binary and discuss the nature and future evolution of the J0106–1000 system. We conclude in Section 5.

2 OBSERVATIONS

We used the 6.5m MMT with the Blue Channel spectrograph to obtain medium resolution spectroscopy of J0106–1000 on UT 2010 Dec 1 – 3. We operate the spectrograph with the 832 line mm^{-1} grating in second order, providing wavelength coverage from 3600 Å to 4500 Å and a spectral resolution of 1.2 Å. We obtain all observations at the parallactic angle, with a comparison lamp exposure paired with every observation. We flux-calibrate using blue spectrophotometric standards (Massey et al. 1988), and we measure radial velocities using the cross-correlation package RVSAO. The details of our data reduction procedures are discussed in Kilic et al. (2009, 2010). We check the stability of the spectrograph using the Hg line at 4358.34 Å from Tucson/Nogales street lights. We measure an average velocity offset of $-0.9 \pm 0.3 \text{ km s}^{-1}$ for this line over the entire three nights of observations.

J0106–1000 is relatively faint ($g = 19.8 \text{ mag}$). We started our observations with 10 min exposures. After detecting $> 400 \text{ km s}^{-1}$ velocity variations in 15 min, we decreased the individual exposure times to 8 min. Realizing that J0106–1000 is a very short period system after our second night of observing, we also acquired high speed photometric observations of J0106–1000 using the McDonald 2.1m Otto Struve Telescope with the Argos frame transfer camera (Mukadam & Nather 2005) on UT 2010 Dec 3. Argos provides a field of view of $2.8' \times 2.8'$. We obtained time series photometry of J0106–1000 with the BG40 filter every 30 s for about 2.6 hr. The Argos field-of-view includes several comparison stars that are useful for relative photometry.

3 RESULTS

3.1 The Orbital Period

Table 1 lists our radial velocity measurements for J0106–1000. We compute best-fit orbital elements using the code of Kenyon & Garcia (1986), which weights each velocity measurement by its associated error. The uncertainties in the orbital elements are derived from the covariance matrix and χ^2 . To verify these uncertainty estimates, we perform a Monte Carlo analysis using 10^4 sets of simulated radial velocities. We adopt the inter-quartile range in the period and orbital elements as the uncertainty.

J0106–1000 exhibits radial velocity variations with a

Table 1. Radial Velocity Measurements for J0106–1000

HJD–2455530 (days)	v_{helio} (km s^{-1})
1.63742	313.3 ± 26.0
1.69330	330.1 ± 24.5
1.74373	116.4 ± 37.5
2.65076	127.9 ± 36.2
2.66124	-292.6 ± 8.8
2.67089	329.7 ± 13.0
2.67802	32.4 ± 16.7
2.68510	-362.4 ± 13.0
2.69110	-146.4 ± 16.7
2.69707	320.9 ± 21.8
2.70401	200.7 ± 18.7
2.70998	-297.8 ± 28.9
2.71774	-132.5 ± 22.7
2.72292	219.2 ± 27.7
2.72909	366.8 ± 26.2
3.63764	-365.2 ± 15.0
3.64378	51.2 ± 17.7
3.65060	384.8 ± 21.0
3.65659	9.3 ± 15.0
3.66333	-402.0 ± 40.2
3.67095	109.9 ± 11.6

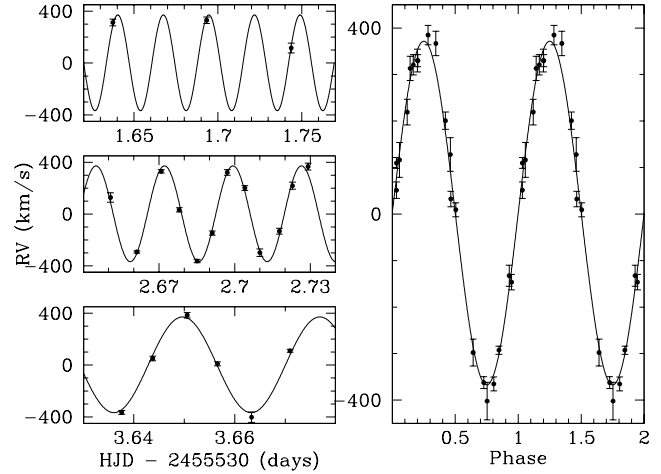


Figure 1. The radial velocities of J0106–1000 observed over three nights in 2010 December (left panels). The right panel shows all of these data points phased with the best-fit period. The solid line represents the best-fit model for a circular orbit with a period of 39.1 min and $K = 369.5 \text{ km s}^{-1}$.

semi-amplitude of $K = 369.5 \pm 3.6 \text{ km s}^{-1}$ and orbital period of $P = 0.027153 \pm 0.0000195 \text{ d}$, or $39.100 \pm 0.028 \text{ min}$. Figure 1 shows the best-fit orbit compared to the observed radial velocities. The relatively long exposure times (8 min) compared to the orbital period (39.1 min) results in an underestimated velocity semi-amplitude, K . This is a direct consequence of the sine curve not being linear when the velocities are at the extremes. To verify this effect, we sampled a sine curve at the exact 21 phases of our observations with $P/5$ long integrations. We recover the exact period, but K is systematically underestimated by 6.5%. Thus, the corrected velocity semi-amplitude for J0106–1000 is $K = 395.2 \text{ km s}^{-1}$. With this correction, J0106–1000 has a mass function

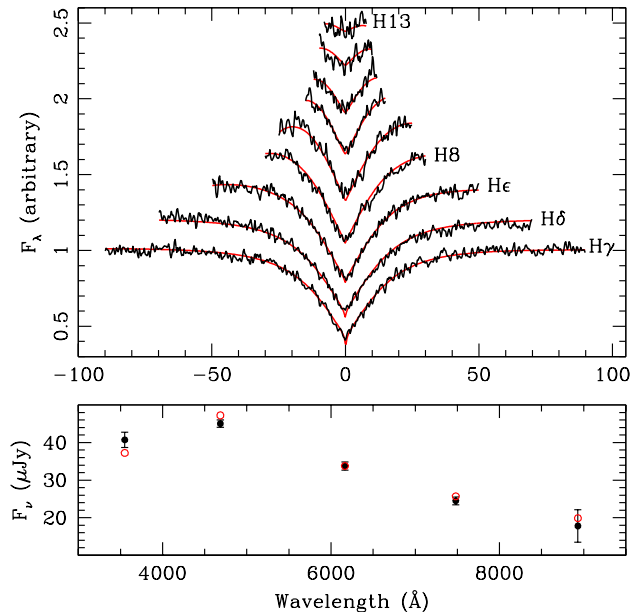


Figure 2. Model fits (red lines) to the Balmer line profiles of J0106–1000 (jagged lines, top panel). The spectral energy distribution of J0106–1000 (based on the SDSS photometry, filled circles) compared to the best-fit model (open circles, bottom panel).

of $f = 0.1736 \pm 0.0047 M_{\odot}$. The systemic velocity (after subtracting the gravitational redshift of 1.9 km s^{-1}) is $0.3 \pm 2.7 \text{ km s}^{-1}$ and the time of spectroscopic conjunction is HJD $2455531.633574 \pm 0.000129 \text{ d}$.

3.2 The Physical Parameters of the Binary

Our time-series spectroscopy provides for robust determinations of effective temperature and surface gravity. We perform stellar atmosphere model fits using synthetic DA WD spectra kindly provided by D. Koester. The grid of WD model atmospheres covers effective temperatures from 6000 K to 30,000 K in steps of 500 K to 2000 K, and surface gravities from $\log g = 5.0$ to 9.0 in steps of 0.25 dex. We perform fits to the Balmer line profiles using the average composite spectra. We also perform fits to the individual spectra to derive a robust statistical error estimate. Figure 2 shows the observed Balmer line profiles (jagged lines) for J0106–1000 compared to our best-fit model (solid line). The best-fit model has $T_{\text{eff}} = 16485 \pm 456 \text{ K}$ and $\log g = 6.01 \pm 0.04$.

Previous stellar atmosphere fits find a comparable $\log g$ but a 2500 K hotter T_{eff} (Kleinman 2010). The discrepancy in their temperature estimate is most likely due to the low signal-to-noise SDSS spectrum. Our best-fit model matches our S/N = 40 spectrum and the SDSS photometry (Figure 2).

Based on the improved Panei et al. (2007) tracks (see Kilic et al. 2010) for ELM WDs, J0106–1000 is a 1.1 Gyr old¹ $0.17 M_{\odot}$ WD with a radius $R = 0.057 R_{\odot}$. Its absolute magnitude $M_g = 7.8$ corresponds to a distance

¹ This age estimate is somewhat uncertain due to the assumption on the thickness of the surface hydrogen layer for $0.17 M_{\odot}$ WDs.

of 2.4 kpc. Based on five epochs from the USNO-B and the SDSS, Munn et al. (2004) measure a proper motion of $(\mu_{\alpha} \cos \delta, \mu_{\delta}) = (20.2, -10.5) \text{ mas yr}^{-1}$. J0106–1000 is 2.3 kpc below the Galactic plane and it has $U = -115 \pm 43$, $V = -222 \pm 43$, and $W = -15 \pm 12 \text{ km s}^{-1}$ with respect to the local standard of rest (Hogg et al. 2005). Clearly, J0106–1000 is a halo star.

The mass function implies a companion mass of $\geq 0.37 M_{\odot}$. The orbit is far too small to contain a main-sequence star of $0.37 M_{\odot}$ or more. Therefore, the companion is a compact object. Based on the mass function alone, the probability of a neutron star ($1.4\text{--}3.0 M_{\odot}$) companion is 7.3%. The probability of a SNe Ia, for which the companion would be a $1.23\text{--}1.40 M_{\odot}$ WD, is only 1.9%. However, if sub-Chandrasekhar mass WDs do explode as Type Ia SNe (van Kerkwijk et al. 2010), this probability may be higher.

3.3 The Light Curve

The chance of an eclipse is relatively high for J0106–1000. For an edge-on orbit, the companion would be a $0.37 M_{\odot}$ WD. To avoid detection in the SDSS photometry, we assume that the companion is $10\times$ fainter than the visible WD and thus it has $T_{\text{eff}} \leq 14600 \text{ K}$ and $R \approx 0.02 R_{\odot}$. The eclipse depth and duration would be 12% and $\approx 90 \text{ s}$ (assuming a total eclipse), respectively. Due to the relatively large size of the visible WD compared to the orbital separation, the probability of a grazing eclipse is 25%.

Figure 3 shows the Argos light curve of J0106–1000 (top panel) over four orbits. J0106–1000 is relatively faint and the Argos light curve has a few percent scatter. We do not detect any pulsations at the $\geq 0.8\%$ level. However, the Fourier transform of the J0106–1000 light curve reveals a significant peak at $1187 \pm 13 \text{ s}$ (half the orbital period) with an amplitude of $1.7\% \pm 0.3\%$. We use the ephemeris from the radial velocity observations obtained on the same night to calculate the phase for our photometric observations. The middle panel in Figure 3 shows the light curve folded over the best-fit orbital period. There are essentially four separate observations every 30 s in the folded light curve. The bottom panel in Figure 3 shows the same light curve binned by four points. This panel clearly shows the ellipsoidal variations; the ELM WD is distorted due to the companion. This is the first detection of ellipsoidal variations for a WD.

To verify that the observed variations in the light curve are not a statistical fluctuation, we perform a bootstrap analysis. We randomly permute the light curve points in time and create 10^5 simulated light curves. This analysis shows that the probability of the measured ellipsoidal variation signal being a random one is smaller than 10^{-5} . We also checked for variations in the brightest reference star by folding its light curve for the 39.1 min period of J0106–1000. This analysis did not reveal any periodic variations in the reference star. These tests show that the detected variability is highly significant.

To model the ellipsoidal variations and the reflection effect, we follow Morris & Naftilan (1993). In their formalism, the amplitude of the ellipsoidal effect is roughly $\delta f_{\text{ell}} = (m_2/m_1)(r_1/a)^3$, where a is the orbital semi-major axis and r_1 is the radius of the primary (Zucker et al. 2007; Shporer et al. 2010). For J0106–1000, $(m_2/m_1) \approx 2.2$ for an edge-on orbit, yielding $\delta f_{\text{ell}} = 1.4\%$. For a more accurate

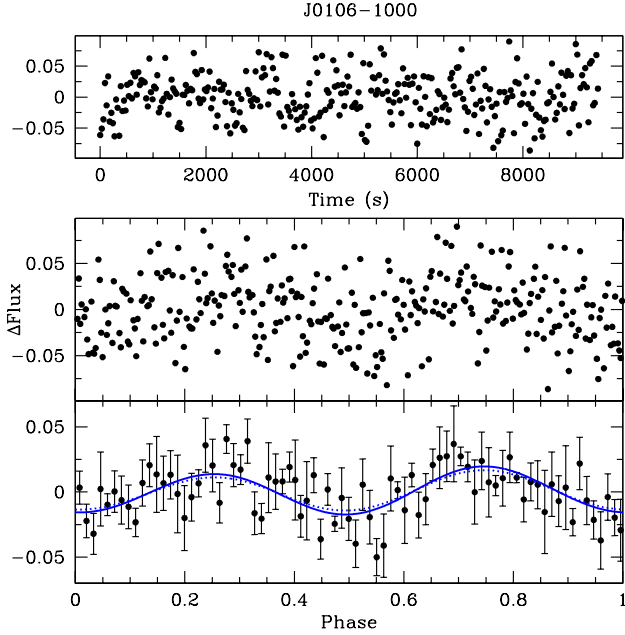


Figure 3. High speed photometry of J0106–1000 over four orbital periods (top panel). The middle and bottom panels show the same light curve folded over the orbital period and binned by four points, respectively. Our best-fit model ($i = 73^\circ$) and a comparable model ($i = 60^\circ$) are shown as solid and dotted lines.

estimate, we follow equation 1 in Morris & Naftilan (1993) and include the low order terms up to the $\cos 4\phi$ term, where $\phi = 0^\circ$ when the primary star is farthest from the observer. The transmission curve of the Argos camera with the BG40 filter is similar to a B -band filter. We use limb darkening and gravity-darkening coefficients of $u_1 = 0.36$ and $\tau_1 = 0.487$, respectively (see equation 1 and Table 1 in Morris & Naftilan 1993). The results change only slightly for different limb-darkening and gravity-darkening coefficients. The ellipsoidal variations are dominated by the $\cos 2\phi$ term, which has an amplitude of 1.8% for the J0106–1000 system at 90° inclination. We estimate the contribution from the reflection effect to be $<0.1\%$ and therefore neglect it. On the other hand, the relativistic beaming effect is expected to be about 0.3% (Maxted et al. 2000; Shporer et al. 2010). We include the beaming effect, but not the eclipses in our calculations.

The amplitudes of the ellipsoidal variations and the relativistic beaming effect depend on the companion mass and orbital separation, which depend on the inclination of the system. Hence, the predicted amplitudes can be represented by a single parameter, the inclination angle. We create model light curves for each inclination angle and chose the model with the least χ^2 as the best-fit model (shown as a solid line in Figure 3). This model has an inclination angle of $i = 73^\circ$ and it matches the phase and amplitude of the variations relatively well. The absence of eclipses in the photometry is also consistent with this inclination angle. The dotted line shows a comparable model with an inclination angle of $i = 60^\circ$. The similarities between the two models and the relatively large scatter in our photometry indicate that the error in inclination is relatively large.

To constrain the inclination angle of the system more accurately, we perform a Monte Carlo analysis where we replace the measured flux f with $f + g \delta f$, where δf is the error in flux and g is a Gaussian deviate with zero mean and unit variance. For each of the 10^5 sets of simulated light curves, we repeat our analysis and find the best-fitting model (and the inclination angle). We adopt the interquartile range as the uncertainty. The Monte Carlo analysis shows that the J0106–1000 light curve is best explained by a model with $i = 67^\circ \pm 13^\circ$. Therefore, the companion is most likely a $0.43M_\odot$ object at an orbital separation of $0.32R_\odot$. The mass ratio of the binary is $q = 0.4$ and the merger time due to gravitational wave radiation is 37 Myr.

4 DISCUSSION

J0106–1000 is the shortest period detached binary WD system currently known. Even though its orbital period is comparable to the AM CVn systems, its spectrum shows only hydrogen absorption lines. There is no evidence of interaction or mass accretion between the two components other than the slight distortion of the ELM WD due to mutual gravitation. The observed ellipsoidal variations are extremely useful for constraining the inclination angle and the masses of both components of the system. The optical spectroscopy and photometry of this system is best explained by a binary system containing two He-core WDs with $M_1 = 0.17M_\odot$ and $M_2 = 0.43M_\odot$ at a separation of $0.32R_\odot$.

The future evolution of the system depends on the mass ratio of the two components. For a mass ratio of $q = 0.4$, J0106–1000 will likely have unstable mass transfer and merge. Dan et al. (2011) simulate the mergers of double degenerate systems including $0.2M_\odot$ ELM WDs with 0.3 – $0.8M_\odot$ WD companions. Their smoothed-particle hydrodynamic models indicate that systems with $q \geq 0.25$ have unstable mass transfer and merge after 20–80 orbits (although see Motl et al. 2007; Racine et al. 2007, for the possibility of stable mass transfer). Unstable mass transfer may also lead to the detonation of the surface helium layer on a C/O WD via Kelvin-Helmholtz instabilities. Guillochon et al. (2010) find that the required conditions for triggering a surface explosion are only achieved in $\geq 0.8M_\odot$ WD accretors with $>0.2M_\odot$ companions. Hence, no efficient carbon burning is expected in binary WD systems containing 0.45 – $0.8M_\odot$ C/O WD accretors and ELM WD donors. Based on these results, J0106–1000 will likely merge and create a $0.6M_\odot$ core-He burning subdwarf in 37 Myr. This mass is close to the canonical mass of $0.5M_\odot$ for subdwarfs (Heber 2009).

Brown et al. (2011) estimate the merger rate of ELM WDs from a complete, color-selected sample of ELM WDs found in the Hypervelocity Star Survey (Brown et al. 2006, 2009). Roughly 5×10^4 (with a factor of few uncertainty) ELM WDs formed in the Galactic disk in the last Gyr. About 70% of these systems merge in less than a Gyr, and 66% of these systems have mass ratios $q \geq 0.25$. From these estimates, roughly 2.3×10^4 ELM WDs merged in the past Gyr. There are three stars with $q \geq 0.25$ and merger times shorter than a Hubble time in their sample. These three stars, J0818+3536, J0923+3028, and J1053+5200, contain 0.17 – $0.23M_\odot + 0.33$ – $0.44M_\odot$ WDs (assuming an average inclination angle of 60°). Based on the evolutionary calcu-

lations by Dan et al. (2011), they are likely to form 0.5–0.67 M_{\odot} single subdwarfs. Hence, the formation rate of single subdwarfs through mergers of ELM WDs is roughly 2.3×10^4 in the last Gyr. Adding J0106–1000 to this sample would increase this rate by about 50% due to its relatively short merger time.

Nelemans (2010) presents population synthesis models for the Galactic population of subdwarf B stars. He predicts a total number of 5.6×10^5 single subdwarfs to form as a result of He WD mergers. The resulting mass distribution is centered around 0.5 M_{\odot} with a tail toward higher masses, similar to the mass distribution of the merger systems discussed above. Hence, the ELM WD merger systems contribute significantly to the population of single subdwarfs in the Galaxy.

Short period binary WDs are important gravitational wave sources. Nelemans et al. (2004) and Roelofs et al. (2007) argue that about half a dozen AM CVn binaries should be detected by LISA. With an orbital period similar to the known AM CVn systems, J0106–1000 may be a promising candidate for detection. The orbital period, inclination, and model-dependent distance estimate for J0106–1000 yield the gravitational wave strain at Earth, $\log h = -22.7$ at a frequency $\log \nu$ (Hz) = -3.07 (Roelofs et al. 2007). This is at the S/N = 1 detection limit of LISA after 1 year of observations. Confusion with Galactic noise sources decreases with accurately known orbital periods. Our ephemeris and orbital period measurements may enable LISA to detect J0106–1000 above the Galactic background noise after a few years of observations.

5 CONCLUSIONS

We discovered the shortest period detached binary WD system currently known. This system also presents the first detection of a tidally distorted WD. We constrain the inclination angle of the system using high-speed photometric observations. J0106–1000 contains a pair of low-mass WDs at an inclination angle of $67^{\circ} \pm 13^{\circ}$. Follow-up high-speed photometric observations at a larger telescope will be useful to better constrain the inclination (and therefore the companion mass) and to search for grazing eclipses. The two WDs will merge in 37 Myr and most likely form a core He-burning single subdwarf star.

ACKNOWLEDGEMENTS

We thank A. Shporer and S. Nissanke for stimulating discussions, D. Koester for kindly providing WD model spectra, and an anonymous referee for useful suggestions. Support for this work was provided by NASA through the *Spitzer Space Telescope* Fellowship Program, under an award from Caltech. KIW, DEW, and JJH gratefully acknowledge the support of the NSF under grant AST-0909107 and the Norman Hackerman Advanced Research Program under grants 003658-0255-2007 and 003658-0252-2009.

REFERENCES

- Bildsten, L., Shen, K. J., Weinberg, N. N., & Nelemans, G. 2007, *ApJ*, 662, L95
- Brown, W. R., Geller, M. J., Kenyon, S. J., & Kurtz, M. J. 2006, *ApJ*, 647, 303
- Brown, W. R., Geller, M. J., & Kenyon, S. J. 2009, *ApJ*, 690, 1639
- Brown, W. R., Kilic, M., Allende Prieto, C., & Kenyon, S. J. 2010, *ApJ*, 723, 1072
- Brown, W. R., Kilic, M., Allende Prieto, C., & Kenyon, S. J. 2011, *MNRAS*, 411, L31
- Dan, M., Rosswog, S., Guillochon, J., & Ramirez-Ruiz, E. 2011, *ApJ*, submitted, arXiv:1101.5132
- Eisenstein, D. J., et al. 2006, *ApJS*, 167, 40
- Guillochon, J., Dan, M., Ramirez-Ruiz, E., & Rosswog, S. 2010, *ApJ*, 709, L64
- Heber, U. 2009, *Annual Review of Astronomy & Astrophysics*, 47, 211
- Hogg, D. W., Blanton, M. R., Roweis, S. T., & Johnston, K. V. 2005, *ApJ*, 629, 268
- Iben, I., Jr., & Tutukov, A. V. 1984, *ApJS*, 54, 335
- Kenyon, S. J. & Garcia, M. R. 1986, *AJ*, 91, 125
- Kilic, M., Brown, W. R., Allende Prieto, C., Swift, B., Kenyon, S. J., Liebert, J., & Agüeros, M. A. 2009, *ApJ*, 695, L92
- Kilic, M., Brown, W. R., Allende Prieto, C., Kenyon, S. J., & Panei, J. A. 2010, *ApJ*, 716, 122
- Kilic, M., Brown, W. R., Allende Prieto, C., Agüeros, M. A., Heinke, C., & Kenyon, S. J. 2011, *ApJ*, 727, 3
- Kleinman, S. J. 2010, *American Institute of Physics Conference Series*, 1273, 156
- Massey, P., Strobel, K., Barnes, J. V., & Anderson, E. 1988, *ApJ*, 328, 315
- Maxted, P. F. L., Marsh, T. R., & North, R. C. 2000, *MNRAS*, 317, L41
- Morris, S. L., & Naftilan, S. A. 1993, *ApJ*, 419, 344
- Motl, P. M., Frank, J., Tohline, J. E., & D’Souza, M. C. R. 2007, *ApJ*, 670, 1314
- Mukadam, A. S., & Nather, R. E. 2005, *Journal of Astrophysics and Astronomy*, 26, 321
- Munn, J. A., et al. 2004, *AJ*, 127, 3034
- Nelemans, G., Yungelson, L. R., & Portegies Zwart, S. F. 2004, *MNRAS*, 349, 181
- Nelemans, G. 2010, *Ap&SS*, 329, 25
- Panei, J. A., Althaus, L. G., Chen, X., & Han, Z. 2007, *MNRAS*, 382, 779
- Racine, É., Phinney, E. S., & Arras, P. 2007, *MNRAS*, 380, 381
- Roelofs, G. H. A., Groot, P. J., Benedict, G. F., McArthur, B. E., Steeghs, D., Morales-Rueda, L., Marsh, T. R., & Nelemans, G. 2007, *ApJ*, 666, 1174
- Sarna, M. J., Marks, P. B., & Connors Smith, R. 1996, *MNRAS*, 279, 88
- Shporer, A., Kaplan, D. L., Steinfadt, J. D. R., Bildsten, L., Howell, S. B., & Mazeh, T. 2010, *ApJ*, 725, L200
- van Kerkwijk, M. H., Chang, P., & Justham, S. 2010, *ApJ*, 722, L157
- Webbink, R. F. 1984, *ApJ*, 277, 355
- Zucker, S., Mazeh, T., & Alexander, T. 2007, *ApJ*, 670, 1326